



Assessment of Creep-Fatigue Endurance of Large Cruciform Weldments

Ian Bretherton¹⁾ and Peter John Budden²⁾

1) *AEA Technology plc, United Kingdom*

2) *British Energy Generation Ltd., United Kingdom*

ABSTRACT Fatigue and creep-fatigue tests on Type 316L(N) austenitic partial-penetration weldments are described. Testing was performed at 550°C under fully-reversed bending with total strain ranges between 0.25% and 1% and hold periods of 0, 1 or 5 hours at maximum strain. Fatigue strength reduction factors of approximately 1.9 were obtained. Simplified crack initiation assessments were carried out using the R5 Procedure and conservatively estimated the specimen endurance. Cyclic elastic-plastic-creep finite element analyses were also performed using a state variable constitutive model and led to conservative but more accurate predictions of weldment endurance.

INTRODUCTION

Components in high-temperature generating plant may be subjected to cyclic loading due to variations in mechanical and thermal loads and periods of steady loading. Moreover, many such components contain welds, which are generally a life-limiting feature under creep-fatigue loading. Weld performance can be influenced by various parameters, such as defects, lack of fusion or penetration, change in component section, differences in material properties across the weld, and residual stresses.

Fatigue design of weldments is generally based on the endurance of the parent metal factored using Fatigue Strength Reduction Factors (FSRFs) derived empirically from test data by comparing parent metal behaviour with that of weldments. At high-temperature, creep-fatigue design methods are included in the ASME (1) and RCC-MR (2) codes. Similarly, R5 (3) enables life assessments of existing plant. However, such methods are less well-validated than

for pure fatigue loading. A comparison of the R5 approach with that in the ASME and RCC-MR codes is given in Budden and Goodall (4). R5 uses a similar classification of weldments into types (dependent on weld geometry and procedure) as that in RCC-MR but into fewer distinct categories. R5 recommends a single value of FSRF for dressed weldments as the FSRF then characterises only the metallurgical notch effect. Distinct values are given for each weld type for undressed welds to cover uncertainties in local geometry. The calculated strain range (Fig.1) for the corresponding homogeneous geometry is multiplied by the FSRF to give the weldment fatigue strain range.

This paper describes a programme of fatigue and creep-fatigue tests on austenitic weldments to validate the advice in R5. The paper summarises the test data and compares the results with R5 assessments based on both elastic and inelastic finite element analyses.

EXPERIMENTAL DETAILS

The material used was 26mm thick solution-annealed Type 316L(N) austenitic steel plate. The plates were cut into 220mm by 900mm pieces and the 220mm edge of the plate given a double-sided vee preparation. A 3mm wide stub was left at the base of the vee to deliberately produce partial penetration welds. Shorter sections of plate, 250mm wide and 100mm long, were cut to form the centre section of the cruciform. The specimen design is shown in Fig.2.

All the austenitic weldments tested were partial-penetration, double-sided, T-butt cruciform fillet welds. The completed welds were dressed so that there was a smooth transition from the parent material to the weld. Each specimen was machined from the welded plates away from the edges to ensure that the run-in and run-out of the weld was not included in the test section.

The tests were performed under fully-reversed four-point bending at constant outer fibre total strain ranges between 0.25% and 1% and a temperature of $550 \pm 3^\circ\text{C}$ using a strain rate of $0.03\% \text{s}^{-1}$. The test rig is shown in Fig.2. Only the active part of the specimen is contained in the furnace. The loading gave a constant radius of curvature and hence outer fibre strain in a homogeneous plain-sided strain-gauged specimen at ambient temperature used for

calibration purposes. The central displacement was subsequently used to control the elevated temperature cruciform weldment tests. Creep dwells of 1h or 5h were applied at maximum outer surface strain by holding the central deflection constant.

The test results are plotted in Fig.3 as total applied strain range against cycles-to-failure. The two highest lines are pure fatigue data and 1h dwell creep-fatigue data, respectively, for the parent plate material. These data are not discussed here. Other lines in Fig.3 show the data for the cruciform weldments under pure fatigue and for 1h and 5h dwells. Further tests are in progress. The effect of increasing the dwell time is to decrease the endurance by increasing the component of total damage due to creep. The fit to the fatigue data for the cruciform specimen represents a FSRF based on nominal strain range of about 1.9 compared with the parent plate data, the FSRF decreasing with increasing strain range.

SIMPLIFIED ANALYSES

Assessments of two tests with total strain ranges of 0.6% and dwells of 1h and 5h, respectively, were performed using simplified R5 methods (3,4). A displacement-controlled elastic two-dimensional finite element analysis of the cruciform specimen was first performed using homogeneous base material properties. The applied displacement was adjusted to give an outer surface strain remote from the weld location of 0.3%. A shakedown analysis to determine the steady cyclic state was not necessary as the extremes of the cycle are equal and opposite. The component did not satisfy strict shakedown. Global shakedown, where at least 80% of each continuous section is within yield in the steady cyclic state, was demonstrated to occur when using the weld value of proof stress but not the lower parent figure. The experiments are thus a severe test of simplified methods. The peak finite element elastic stresses are close to the commencement of the blend radius between the plate and the stub (Fig.2). It is argued, for purposes of analysis, that the local singularity due to the unfused land may be neglected since the unfused land is remote from the critical location and close to the neutral bending axis. The R5 approach for dressed welds (which includes F-stresses) is then followed. The thickness correction factor of $(t/22)^{0.25}$ as recommended in R5 (3) applied to the nominal FSRF of 1.5 gives a nett FSRF of 1.564.

The fatigue strain range ($\Delta\epsilon$), the start-of-dwell stress (σ_{ref}^s) and the elastic follow-up factor (Z) at the assessed location are required for an R5 assessment. Estimates of $\Delta\epsilon$ and σ_{ref}^s are first made based on parent material data. The details of the modifications for weldments are described in Budden and Goodall (4). Z is taken as 1.25 from a parent material elastic-creep analysis. The calculations of stress and strain range for the base material can be performed using two different methods in the present case where the dwell is at the peak C of the hysteresis loop in Fig.1. The simpler route is to first estimate the stress drop $\Delta\sigma_{rD}$ during the dwell CD based on relaxation data from σ_{ref}^s , in this case the elastic stress at C. Starting from the elastic stress range at C enhanced by $\Delta\sigma_{rD}$, the Neuber method in conjunction with the cyclic stress-strain data then determines the strain range. The second and generally less conservative approach approximately constructs the two half-cycles ABCD and DEF (Fig.1) and takes the maximum of the two as the fatigue strain range. The start-of-dwell stress σ_{ref}^s is limited to 1.5 times the yield stress in both approaches. An additional volumetric strain correction is also added in both cases. The calculated strain range is then multiplied by the FSRF to give $\Delta\epsilon$ for the weldment.

The fatigue damage per cycle is given by $d_f = 1/N(\Delta\epsilon)$ where $N(\Delta\epsilon)$ is the parent material endurance at strain range $\Delta\epsilon$. No size correction to the Type 316 endurance data used is required as the 26mm thick section is large compared with conventional endurance specimens. The creep damage per cycle is conservatively taken as $d_c = Z\Delta\sigma_{rD}/E\epsilon_L$ where the uniaxial creep ductility ϵ_L is taken as a constant 14%. Total damage per cycle is then $d_t = d_f + d_c$ and the estimated cycles to crack initiation is $1/d_t$. The normalised estimates of endurance based on saturated cyclic data are listed in Table 1 and can be seen to be conservative. Both methods of determining $\Delta\epsilon$ were used and are covered by the range of results in Table 1. The second route generally gave the higher estimates of endurance. The ranges given also cover various assumptions for the uniaxial stress relaxation behaviour in the absence of cast-specific data. The predicted ranges of d_c/d_f are included in Table 1. It can be seen that the creep component of total damage is calculated to be significant for both the 1h and 5h dwells. It should be noted, however, that the estimated lives correspond to initiation of a macroscopic defect whereas the test data correspond to complete specimen failure. Conservatism would be reduced if the crack propagation phase were separately assessed.

INELASTIC ANALYSES

Inelastic finite element analyses at 0.4, 0.6 and 1% total strain ranges were performed using the Fast Reactor State Variable (FRSV) constitutive model (5) within a user subroutine for ABAQUS (6). The FRSV model is a classical state variable description in that it considers plastic and creep strains separately. Parameters in the FRSV model obtained for Type 316 material were used. Time-independent plasticity and creep effects were considered. Plane strain 2D results for a test case were close to those from a 3D analysis and hence plane strain was used to simulate the strain-controlled cyclic tests. The finite element mesh contained 848 eight-noded bi-quadratic elements with 2705 nodes.

The maximum fatigue strain range and creep strain were determined from cyclic inelastic finite element analyses for the applied strain ranges (Table 1) at the steady cyclic state. In each case the maximum was in the parent plate material close to the blend radius. The computed strain range was then multiplied by the FSRF of 1.564. The computed creep strain is not factored for this material (3). The estimated endurance then follows from the linear damage summation rule using best-estimate parent fatigue data (Fig.3) and a parent creep ductility of 60% or 14%, for strain rates greater than 10^{-3}s^{-1} or less than 10^{-5}s^{-1} , respectively. Intermediate ductilities are taken as linear with $\log(\text{strain rate})$. The results are listed in Table 1 normalised by the corresponding test data. It can be seen that the estimated endurances are conservative with respect to the data but tend to be higher than those calculated using the simplified approach. The ratios d_c/d_f are also included in the table. The contribution of creep to the total damage is estimated to be lower than that from the simplified elastic route for the two creep-fatigue tests at 0.6% total strain range. As for the simplified assessments, the estimated lives correspond to initiation of a macroscopic defect whereas the test data correspond to complete specimen failure.

CONCLUSIONS

Creep-fatigue bend tests at 550°C on Type 316L(N) austenitic cruciform partial-penetration weldments have been described. The tests were performed at total applied strain ranges of between 0.25% and 1% with dwell times of 0, 1h and 5h at maximum strain. Measured endurance reduced with increasing strain range and dwell time. An experimental Fatigue

Strength Reduction Factor of about 1.9 was obtained based on nominal strain range but tended to decrease with increasing strain range. Assessments of crack initiation using the R5 procedure and based on both simplified elastic and detailed inelastic finite element analyses have also been described. Conservative assessments of cycles to failure were obtained.

ACKNOWLEDGEMENT

This paper is published with permission of British Energy Generation Ltd. and AEA Technology plc. The authors thank Mr P. Booth for assistance with the calculations.

REFERENCES

1. ASME III, Rules for Construction of Nuclear Power Plant Components, Division 1 Sub-section NH, Class 1 Components in Elevated Temperature Service, ASME, 1995.
2. RCC-MR, Design and Construction Rules for Mechanical Components of FBR Nuclear Islands, AFCEN, Paris, 1985; also Addendum 1, 1987.
3. R5: Assessment Procedure for the High Temperature Response of Structures, Issue 2, British Energy plc, Gloucester, UK, 1998.
4. Budden, P.J. and Goodall, I.W., "Assessment Procedures and Design Codes", *Proc. Conference on Integrity of High-Temperature Welds*, pp309-322, IOM/IMEchE, London, 1998.
5. White, P.S., Hübel, H., Wordsworth, J. and Turbat, A., Guidance Document for the Choice and Use of Constitutive Equations in Fast Reactor Analysis, Final Report on CEC Contract RA1-0164-UK, 1994.
6. ABAQUS User Manual, Version 5.5, Hibbitt, Karlsson and Sorenson Inc., 1995.

Table 1. Ratios of Estimated to Actual Test Endurances and Estimated Creep Damage to Estimated Fatigue Damage for the Cruciform Weldment Tests.

		Simplified Analysis		Inelastic Analysis	
Total Strain Range (%)	Dwell Time (h)	Ratio of Estimated to Test Endurance	Estimated Ratio d_c/d_f	Ratio of Estimated to Test Endurance	Estimated Ratio d_c/d_f
1.0	0	-	-	0.14	-
1.0	1	-	-	0.21	0.065
1.0	5	-	-	0.43	0.077
0.6	0	-	-	0.31	-
0.6	1	0.13-0.31	0.59-2.38	0.61	0.21
0.6	5	0.11-0.32	0.73-2.75	0.65	0.24
0.4	0	-	-	0.15	-
0.4	1	-	-	0.69	1.22

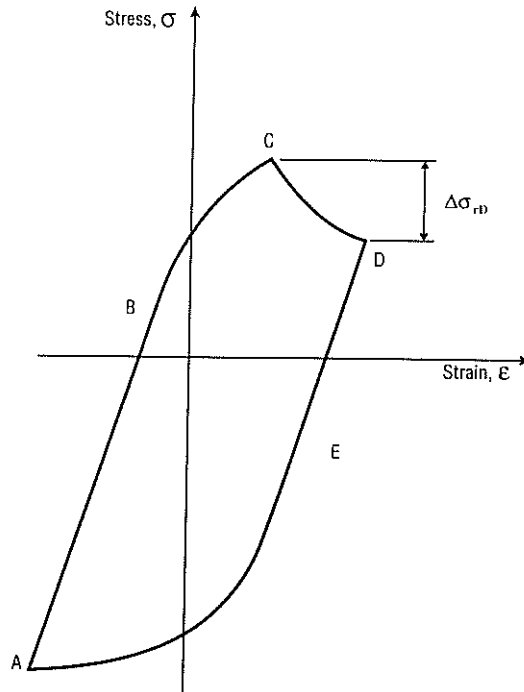


Figure 1. Schematic Creep-Fatigue Hysteresis Loop - Dwell at Cycle Peak

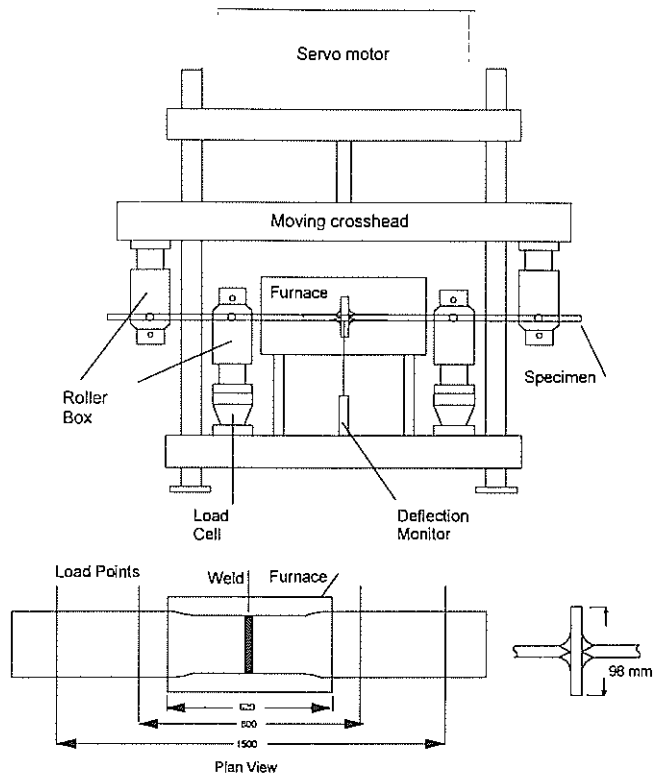


Figure 2. Cruciform Specimen and Test Rig

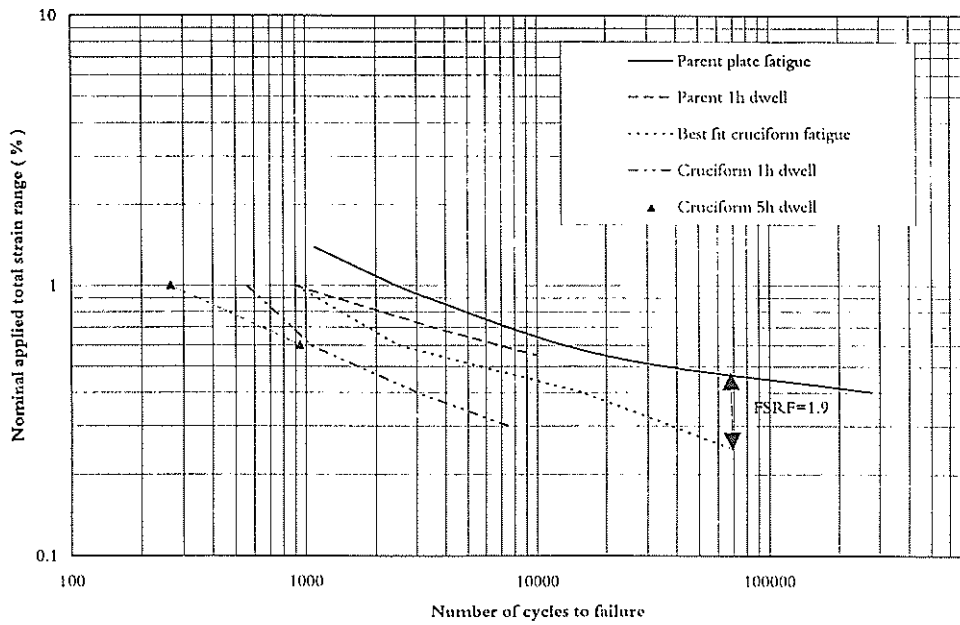


Figure 3. Base Material and Cruciform Weldment Test Data